



Prediction of Shear Wave Velocity by Extreme Learning Machine Technique from Well Log Data

Meysam Rajabi ^{1*}, Hamzeh Ghorbani ², Saeed Khezerloo-ye Aghdam ³

1. Department of Mining Engineering, Birjand University of Technology, Birjand, Iran
2. Young Researchers and Elite Club, Ahvaz Branch, Islamic Azad University, Ahvaz, Iran
3. Department of Petroleum Engineering, Amirkabir University of Technology, Tehran, Iran

Received: 06 August 2021; Accepted: 12 January 2022

DOI: 10.22107/jpg.2022.298520.1151

Keywords

Shear Wave Velocity
ELM
MLP
Machine Learning
Well log data

Abstract

Shear wave velocity (V_s) is one of the key geomechanical parameters effective in the drilling of hydrocarbon reservoirs. In this study, a novel machine learning (extra learning machine (ELM)) approach is developed to predict V_s based on four input variables obtained from well log, including neutron porosity (NPHI), bulk density (RHOB) and gamma-ray (GR). Two algorithms multi-layer perceptron (MLP) and ELM and various empirical equations (Brocher, Eskandari et al., Castagna et al. and Pickett) have been used to predict V_s in this paper. The results show that the performance accuracy for these models includes: ELM > MLP > Castagna et al. > Eskandari et al. > Pickett > Brocher. So, the result that shows the ELM model has higher accuracy than the other machine learning (MLP) approach and also other empirical equations (RMSE = 0.0444 km/s and $R^2 = 0.9809$). Some advantages to the other artificial neural network approach include higher accuracy and performance characteristics, simple algorithm learning, improved performance, nonlinear conversion during training, no stuck in local optimal points, and it is over fitting. The novelty used in this paper is the type of newly implemented artificial model (ELM) and the number of input parameter. This approach possesses to the higher power, speed and accuracy than the methods used by other researchers to predict V_s .

4.1. Introduction

Determination of shear wave velocity (V_s) is one of the key factors in the drilling operation design. Reservoir geomechanics is an important parameter in drilling engineering applications. It fully discloses the mechanical behavior of rocks in subsurface stress and predicts the movement potential (Kaviani-Hamedani et al., 2021; Rhett, 1998; Wang, 2000) it is an important parameter to reduce operating costs during drilling or maintenance. Hydrocarbon wells are known as a threat to their survival (Hudson et al., 2005; Sohail and Hawkes, 2020).

The accuracy of developed geomechanical models depends on reliability of data obtained

from mechanical tests on core samples taken from subsurface formations (Khoshouei and Bagherpour, 2021; Miah et al., 2021). Due to the high cost of coring operations, few oils or gas field wells are candidates for coring operation, which adverse feed data accessibility for researchers. Many empirical correlations have been developed based on petrophysical survey data to eliminate this shortcoming (Sohail et al., 2020).

One of the most important parameters related to the petrophysical evaluation of rock is the shear wave velocity (V_s), which can be implemented to estimate the mechanical properties of the rock according to the compressional-wave velocity, bulk density,

and this parameter (Du et al., 2019; Elkatatny et al., 2018; Parvizi et al., 2015; Tixier et al., 1975).

The basic element in construction of empirical relationships is accessibility to the shear wave velocity parameter obtained from Lab studies (Anemangely et al., 2019). For reasons of cost reduction and the non-mandatory application of geomechanical considerations in the design and completion of older wells, most of the petrophysical survey data collected from the wells did not involve the use of an advanced sonic dipole plot (DSI) (Najibi et al., 2015; Wang et al., 2019).

In addition to empirical methods and tools, experimental methods can also be used as a simple method for predicting V_s (Akhundi et al., 2014). Some researchers such as Brocher (2005), Eskandari et al. (2003), Castagna et al. (1993) and Pickett (1963) presented experimental equations to determine V_s based on a relationship with compressional wave velocity (V_p), as shown in Table 1. However, one of the problems with experimental methods is that they cannot achieve the desired results (Akhundi et al., 2014).

Several studies in artificial intelligence techniques have been conducted to determine oil and gas reservoirs' geomechanical properties and key parameters. All these studies show that artificial intelligence methods have a higher performance, and accuracy when experimental regressions are available (Bagheripour et al., 2015; Behnia et al., 2017; Oloruntobi and Butt, 2020; Seifi et al., 2020). Many researchers have predicted V_s using artificial intelligence, listed below and reported in Table 2 (best algorithm show with star).

In 2007, Rezaei et al., predicted V_s according to three algorithms of fuzzy logic (FL), artificial neural network (ANN), and adaptive neuro-fuzzy inference (ANFIS) based on 637 data sets of 5 input variables including neutron porosity (NPHI), bulk density (RHOB), Gamma-ray (GR), true resistivity (RT), and V_p . This study shows that the best algorithm in this intend is FL, which has a computational

error for this algorithm, including $R^2 = 0.946$ and $MSE = 0.051$ (Rezaee et al., 2007).

In 2010, Rajabi et al., predicted V_s based on three algorithms of genetic algorithm (GA), FL, ANFIS according to 3030 data sets of 3 input variables including NPHI, RHOB and RT. This study shows that the best algorithm is FL, which has a computational error of $MSE = 0.0148$ and $R^2 = 0.951$ (Rajabi et al., 2010).

In 2015, Bagheri pour et al., constructed a model to predict V_s according to the support vector regression (SVR) algorithm based on information related to 4055 data sets of 7 input variables including RHOB, GR, photoelectric absorption factor (PEF), DT, RT, Shallow resistivity (R_s) and NPHI was used. This study shows that the computational error network for this algorithm includes $RMSE = 0.0733$ and $R^2 = 0.971$ (Bagheripour et al., 2015).

In 2019, Mehrgini et al. predicted V_s based on four algorithms of Elman neural network (ENN), ENN-PSO, multilayer perceptron (MLP), MLP-PSO based on information on 760 data sets of 5 input variables RT, ROHB, GR, NPHI and VP were used. This study shows that the computational error log for this algorithm includes $RMSE = 0.0636$ and $R^2 = 0.914$ (Mehrgini et al., 2019).

In 2019, Anemangely et al. constructed a model to predict V_s on the basis of four algorithms LSSVM-GA, LSSVM-PSO, and LLSVM-COA based on information about 3674 data sets, 5 input variables including GR, RT, NPHI, RHOB, and VP were used. This study shows that the computational error log for the best algorithm (LLSVM-COA) algorithm includes $RMSE = 0.073$ and $R^2 = 0.929$ (Anemangely et al., 2019).

In 2020, Wood used six input variables, including GR, RHOB, NPHI, DPHI, RT, and VP, to predict V_s by 3 algorithms of transparent open box (TOB), TOB-GRG, and TOB-Firefly, based on data from 1000 data sets. This study shows that the computational error for the best algorithm (TOB-GRG) includes $RMSE = 11.08$ and $R^2 = 0.9999$ (Wood, 2020).

In 2020, Wang et al. predicted V_s according to

four algorithms TOB, TOB-GRG, and TOB-Firefly based on 2369 data from 6 input variables including RHOB, Cal, CNL, GR, DT, PERM, RS, RT, SP, and VP. This study shows that the computational error for the best algorithm (GRG) includes RMSE = 0.0917 and $R^2 = 0.990$ (Wang et al., 2020).

In this research, based on 6,000 data sets collected from three wells located in south west of Iran, and also based on the new extreme machine learning (ELM) algorithm, a new algorithm is developed with good performance

characteristics.

ELM is a neural network technique for statistical classification, regression analysis, clustering, approximation, comparison and training of the properties of a single layer or multilayer in a hidden node. Therefore, hidden node parameters are not mandatory. ELM advantages and features include precision and performance, simple learning algorithm, improved performance, non-linear conversion during training, no blocking at local sweet spots and overfitting.

Table 1. Published common empirical correlations used to predict shear wave velocity (VS).

Researcher(s)	Proposed equations
Brocher, (2005)	$V_s = 0.7858 - 1.2344V_p + 0.7949V_p^2 - 0.1238V_p^3 + 0.0064V_p^4$
Eskandari et al. (2003)	$V_s = -1.1236V_p^2 + 1.61V_p - 2.3057$
Castagna et al. (1993)	$V_s = 1.0168V_p - 0.05509V_p^2 - 1.0305$
Pickett, (1963)	$V_s = V_p/1.9$

Table 2. List of researchers who researched based on different methods of artificial intelligence to predict Vs.

Work	Data collection	Data description		Techniques	Statistical Error*
		Input variables			
Rezaei et al., (2006)	637	NPHI, RHOB, GR, RT, and VP		FL*, ANN, and ANFIS	$R^2 = 0.946$, MSE = 0.051
Rajabi et al., (2010)	3030	RHOB, RT, and NPHI		GA, FL*, ANFIS	MSE = 0.0148, $R^2 = 0.951$
Bagheri pour et al. (2015)	4055	RHOB, GR, PEF, DT, RT, RS and NPHI		SVR	RMSE = 0.0733, $R^2 = 0.971$
Mehrgini et al., (2019)	760	RT, ROHB, GR, NPHI, and VP		ENN*, ENN-PSO, MLP, MLP-PSO	RMSE = 0.0636, $R^2 = 0.914$
Anemangely et al., (2019)	3674	GR, RT, NPHI, RHOB, and VP		LSSVM-GA, LSSVM-PSO, and LLSVM-COA*	RMSE = 0.073, $R^2 = 0.929$
Wood, (2020)	1000	GR, RHOB, NPHI, DPFI, RT, and VP		TOB, TOB-GRG*, and TOB-Firefly	RMSE = 11.08, $R^2 = 0.9999$
Wang et al., (2020)	2369	RHOB, Cal, CNL, GR, DT, PERM, RS, RT, SP, and VP		PSO-LSTM*, LSTM, and RNN	RMSE = 0.0917, $R^2 = 0.990$

4.2. Material Method

2.1. Workflow Diagram

In Figure 1, the workflow for Vs prediction using both MLP and ELM algorithms is shown. According to Figure 1, for the first step, the data are collected, then to normalize the data, we determine their maximum and minimum and then normalize the data. In the next step, we divide the data into two parts: training and

testing. Finally, we run the models and, after comparing the models using statistical parameters, identify the best algorithm and present the results.

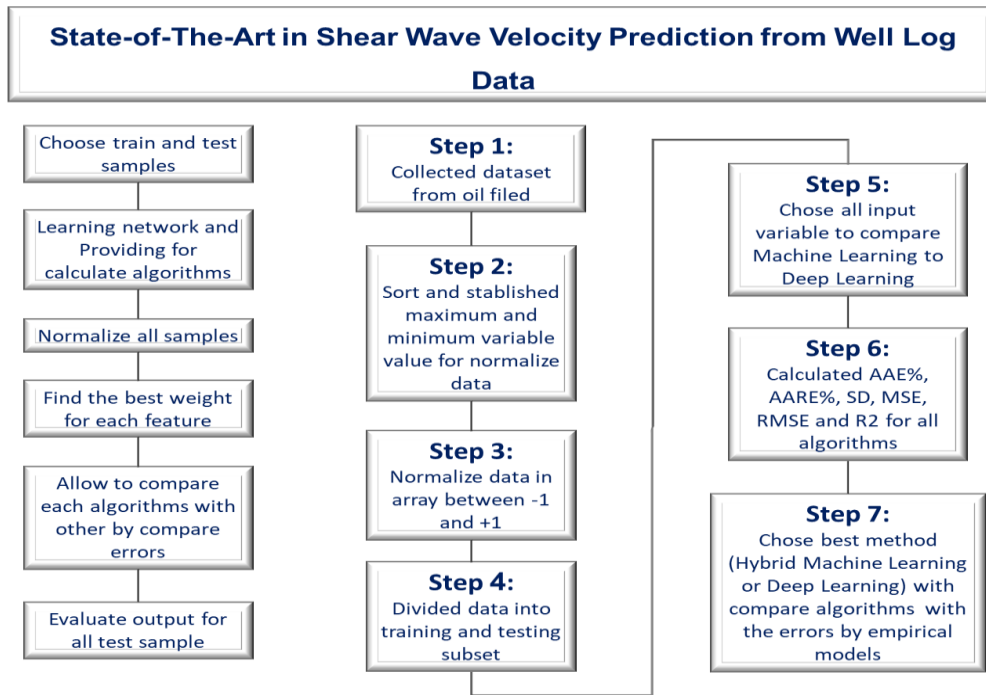


Figure 1. Flow diagram for shear wave velocity prediction.

2.2. Machine Learning Algorithm

Today, machine learning algorithms are widely used as a powerful tool for accurately predicting key parameters of the oil and gas industry with other influential variables. (Choubineh et al., 2017; Ghorbani et al., 2017; Ghorbani et al., 2020; Ghorbani et al., 2018; Ghorbani et al., 2019).

In this study, two powerful machine learning algorithms with powerful multilayer perceptron (MLP) and extreme learning machine (ELM) have been used to develop and predict V_s with high accuracy and investigate them; these algorithms with experimental equations We compare.

2.2.1. Multilayer Perceptron Algorithm

Artificial neural networks (ANN) is one of the methods to facilitate accurate prediction of dependent variables and complex methods and equations (Ali, 1994) that, due to the variety of complexities of each dependent variable, presented different types of neural networks (Ghorbani et al., 2019). Reasons that increase

the accuracy of the operation include selecting features (i.e., input variables to be considered), network architecture (number of layers and nodes) and the transfer of functions between layers, and the choice of the training algorithm. We use Multi-Layer Perceptron (MLP) to increase performance accuracy in artificial intelligence networks. One of the on-train algorithms that assist the MLP algorithm in fast optimization convergence is the Levenberg-Marquardt (LM) algorithm built into this algorithm. For further study of this algorithm, refer to Ghorbani et al. (2018); Mohamadian et al. (2021) articles (Ghorbani et al., 2018; Mohamadian et al., 2021).

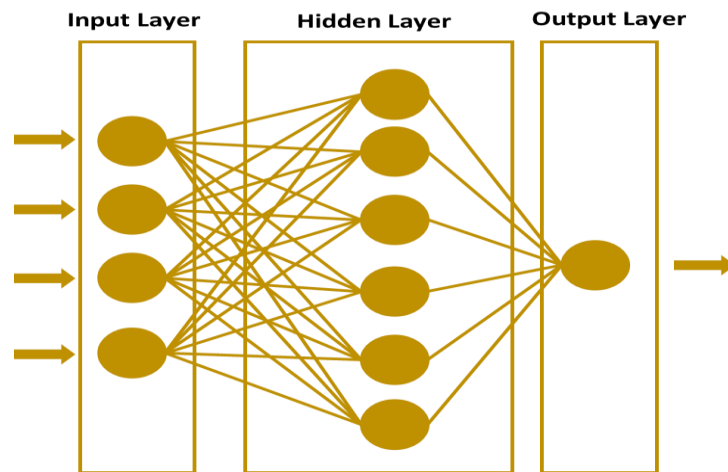


Figure 2. Schematic of MLP for shear wave velocity prediction.

2.2.2. Extreme Learning Machine (ELM) Algorithm

Extreme learning machine (ELM) is one of the fastest neural networks that can reduce learning time, improve accuracy and increase generalizability (Cheng and Xiong, 2017; Huang, 2014). This algorithm is completely different from the ANN algorithm. It uses other optimization or diffusion algorithms because all the internal learning parameters of the ELM are randomly determined, which saves computational time. During the ELM training, the parameters of the hidden layer (weight and

bias) do not need to be adjusted. In this algorithm, the output weight is determined using the random from a uniform inverse function to the hidden layer for the output matrix (Yeom and Kwak, 2017). The structure of a simple ELM (with a single hidden layer) is shown in Figure 3. To study more of this algorithm and also to reduce the additional content and study its exact structure, refer to the articles of previous researchers includes Rashidi et al. (2021); Yeom and Kwak, 2017 and Huang et al., 2011 (Huang et al., 2011; Rashidi et al., 2021; Yeom and Kwak, 2017).

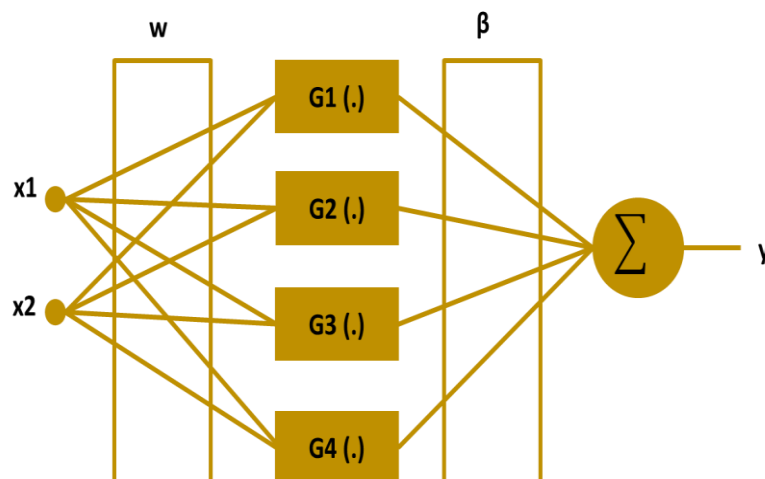


Figure 3. Schematic of single hidden layer for extreme learning machine (ELM) (Yeom and Kwak, 2017).

4.3. Data Gathering

In this article, data gathered from three wells (wells #A, #B and #C) belonged to one of the oil fields in southwestern Iran. Wells #A and #B information was used for modelling, and wells #C information was used to validate the model. The information is for well # B (967 data records) the depth interval 3316 to 3538 m, well # A (942 data records) the depth interval 3345 to 3533 m and well # C (971 data records) the depth interval 3279 to 3473 m. The statistical parameters related to these wells are reported in Table 3.

To construct artificial intelligence models and compare them with experimental equations, data related to well #A and #B (1909 data records) have been used to validate well #C (971 data records).

The main reason for choosing two wells A and B for modeling for algorithms is that the data

range in the two wells is wider than the C # well. Therefore, the best choice was to select two wells #A and #B as modeling and the well # C is selected as validation.

1909 data sets are related to wells #A and #B, of which 70% (1336 data sets) are for training and 30% (572 data sets) for testing. Neutron porosity (NPHI); bulk density (RHOB); surface resistivity (RES-SHT); compression wave velocity (Vp); average resistivity (RES-MED); gamma rays (GR); deep resistivity (RES-DEP), and gauge (CP) were the variables studied in this paper. This data has been used as input variable data for artificial intelligence. For validation of the algorithm, we used well #C. Table 3 shows statistical details obtained by SPSS software for total data for well #A, well #B, and #C.

As can be seen in this table, the data scatter for wells #A and #B is greater than wells #C.

Table 3. Statistical characterization of data variables for all complete data (well #A, #B and #C).

<i>Parameters</i>		<i>Compressio nal-Wave Velocity</i>	<i>Gamma Ray</i>	<i>Bulk Density</i>	<i>Neutr on</i>	<i>Shallow Resistivity</i>	<i>Medium Resistivity</i>	<i>Deep Resistivity</i>	<i>Caliper</i>	<i>Shear wave velocity</i>
-	<i>Symbol</i>	<i>Vp</i>	<i>GR</i>	<i>RHOB</i>	<i>NPHI</i>	<i>RES-SHT</i>	<i>RES-MED</i>	<i>RES-DEP</i>	<i>CP</i>	<i>Vs</i>
-	<i>Units</i>	<i>km/s</i>	<i>GRAPI</i>	<i>g/cc</i>	<i>PU</i>	<i>Ohms-m</i>	<i>Ohms-m</i>	<i>Ohms-m</i>	<i>Inches</i>	<i>km/s</i>
Well #A	<i>Mean</i>	4.21	42.93	2.51	15.73	4.73	3.72	4.45	8.62	2.32
	<i>Std. Deviation</i>	0.58	61.77	0.12	10.07	89.47	2.63	51.42	0.04	0.33
	<i>Variance</i>	0.34	3815.10	0.01	101.3	8003.07	6.89	2643.24	0.00	0.11
	<i>Minimum</i>	2.71	1.04	2.16	3.28	0.20	0.19	0.23	8.47	1.40
	<i>Maximum</i>	5.19	316.27	2.93	54.65	5464.37	29.49	2189.60	8.87	3.15
Well #B	<i>Mean</i>	4.21	56.23	2.56	14.77	3.84	25.50	3.85	8.63	2.32
	<i>Std. Deviation</i>	0.46	60.24	0.07	8.45	2.79	908.59	3.05	0.03	0.30
	<i>Variance</i>	0.21	3627.25	0.00	71.32	7.79	825241.98	9.33	0.00	0.09
	<i>Minimum</i>	2.72	5.67	2.21	4.23	0.71	0.14	0.70	8.50	1.46
	<i>Maximum</i>	5.09	587.02	2.70	54.35	14.34	46224.45	15.07	8.77	2.94
Well #C	<i>Mean</i>	4.63	10.02	2.57	9.39	4.53	4.67	4.71	8.58	2.49
	<i>Std. Deviation</i>	0.31	3.22	0.05	3.11	2.63	2.64	2.88	0.01	0.16
	<i>Variance</i>	0.10	10.36	0.00	9.65	6.90	6.99	8.31	0.00	0.03
	<i>Minimum</i>	4.13	4.16	2.48	2.90	2.16	2.09	2.18	8.55	2.15
	<i>Maximum</i>	5.41	24.84	2.66	14.48	13.36	14.42	14.08	8.63	2.87

4.4. Result and Discussion

4.1. Feature Selection

One of the methods used to increase the speed, efficiency and accuracy of performance is the feature selection method. When the number of input variables is high, this method leads to the best estimate of the performance of the inputs and avoids consecutive repetitions. In this article, the filtering method is used. This method has a higher speed and accuracy of performance than other methods. In this method, the MLP algorithm is used. Using the GA algorithm, first, the control parameters are determined. The high-performance solutions (minimum RMSE) are transferred to the next optimizer iteration, then using the MLP network, this minimum RMSE applies new iterations. This allows it to select features with less RMSE for each input category and select the best result from these input combinations. The feature selection process is as follows: First, the features are selected into categories of one, two, three, etc., up to eight. In the next step, for example in the first category, enter each feature as input to the MLP-GA algorithm and after outputting the RMSE value is obtained for them. Finally, the best RMSE is reported in Table 5. This comparison shows that the most effective input feature among the categories is Vp. For this purpose, all the data in the article have been used for feature selection.

The main purpose of this method is to select and determine the optimal combination of the nine input variables (characteristics) listed in

Table 4.

Table 4. Catechization of input variables and symbol code.

<i>Input Variable</i>	<i>Symbol Code</i>
<i>Vp</i>	<i>Z1</i>
<i>RES-DEP</i>	<i>Z2</i>
<i>RHOB</i>	<i>Z3</i>
<i>CP</i>	<i>Z4</i>
<i>NPHI</i>	<i>Z5</i>
<i>RES-SHT</i>	<i>Z6</i>
<i>RES-MED</i>	<i>Z7</i>
<i>GR</i>	<i>Z8</i>

The results of this feature selection are shown in Table 5 and Figure 4. The information in this table in Figure 4 and Table 5 shows that the error value for the four inputs has a greater effect on predicting the Vs value, including Vp, RHOB, NPHI and GR.

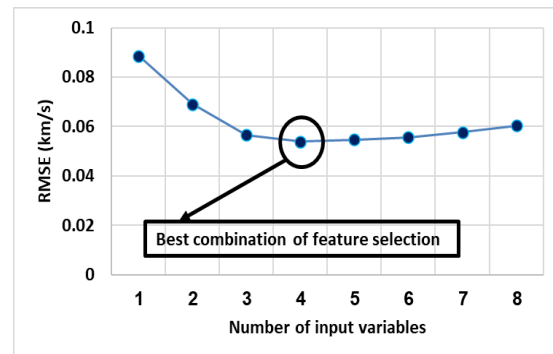


Figure 4. RMSE versus number for the combination of input variables.

Table 5. Feature selection for combination input variables.

<i>Number of input variables</i>	<i>Input variables</i>	<i>RMSE (km/s)</i>
1	<i>Z1</i>	0.0887
2	<i>Z1, Z5</i>	0.0690
3	<i>Z5, Z1, Z8</i>	0.0567
4	<i>Z3, Z8, Z5, Z1 (Best)</i>	0.0539
5	<i>Z8, Z5, Z1, Z7, Z3</i>	0.0547
6	<i>Z7, Z3, Z8, Z5, Z1, Z6</i>	0.0556
7	<i>Z6, Z1, Z7, Z3, Z5, Z8, Z2</i>	0.0576
8	<i>Z1, Z5, Z6, Z4, Z3, Z7, Z2, Z8</i>	0.0605

4.5. Error Parameters & Discussion

For comparison, the machine learning (ELM and MLP) and empirical equations (Brocher, Eskandari et al., Castagna et al., Carroll and Pickett) we used; measures are percentage deviation (PD_i), average relative error (ARE),

$$PD_i = \frac{\xi_{(Measured)} - \xi_{(Predicted)}}{\xi_{(Measured)}} \times 100 \quad (1)$$

$$ARE = \frac{\sum_{i=1}^n PD_i}{n} \quad (2)$$

$$AARE = \frac{\sum_{i=1}^n |PD_i|}{n} \quad (3)$$

$$SD = \sqrt{\frac{\sum_{i=1}^n (D_i - D_{imean})^2}{n-1}} \quad (4)$$

$$D_{imean} = \frac{1}{n} \sum_{i=1}^n (\xi_{Measured_i} - \xi_{Predicted_i})$$

$$MSE = \frac{1}{n} \sum_{i=1}^n (\xi_{Measured_i} - \xi_{Predicted_i})^2 \quad (5)$$

$$RMSE = \sqrt{MSE} \quad (6)$$

$$R^2 = 1 - \frac{\sum_{i=1}^N (\xi_{Predicted_i} - \xi_{Measured_i})^2}{\sum_{i=1}^N (\varphi_{Predicted_i} - \frac{\sum_{i=1}^n \xi_{Measured_i}}{n})^2} \quad (7)$$

average absolute relative error (AARE), standard deviation (SD), mean square error (MSE), root mean square error (RMSE), and coefficient of determination (R²). The computation formulas for these statistical measures are expressed in Equation (1) to Equation (7).

Since 1909, the data is related to wells #A and #B. 70% of the data is related to training. The remaining 30% is testing. After modelling using artificial intelligence algorithms (MLP and ELM) and using empirical equations (Brocher, Eskandari et al., Castagna et al. and Pickett), information about training and testing and the total is given in Tables 6, 7 and 8.

As shown in the results of Tables 6 to 8, based on a comparison between artificial intelligence algorithms and empirical equations, we conclude that the performance accuracy of artificial intelligence algorithms is higher than empirical equations. The comparison between the models shows that ELM has higher performance accuracy than other empirical equations and MLP.

Based on the results in these tables, it is

determined that for educational data the values of AARE% = 1.351 and RMSE = 0.0409 km / s and for test data these values include AARE% = 1.628 and RMSE = 0.0518 km / s and for the total Data include AARE% = 1.434 and RMSE = 0.0444 km / s.

Table 6. Accuracy achieves for shear wave velocity prediction applied to the training dataset (70% of the total dataset).

<i>Models Unit</i>	<i>ARE%</i> (%)	<i>AARE%</i> (%)	<i>SD</i> (km/s)	<i>MSE</i> (km/s)	<i>RMSE</i> (km/s)	<i>R²</i> -
<i>Pickett</i>	4.139	5.073	0.1562	0.0244	0.1563	0.8503
<i>Castagna et al.</i>	2.448	4.126	0.1312	0.0172	0.1312	0.8504
<i>Eskandari et al.</i>	2.754	4.488	0.1402	0.0196	0.1401	0.8503
<i>Brocher</i>	-4.266	7.759	0.2045	0.0418	0.2045	0.8506
<i>MLP</i>	-0.157	1.535	0.0477	0.0023	0.0477	0.9735
<i>ELM</i>	-0.085	1.351	0.0408	0.0017	0.0409	0.9846

Table 7. Accuracy achieves for shear wave velocity prediction applied to the testing dataset (30% of the total dataset).

<i>Models Unit</i>	<i>ARE%</i> (%)	<i>AARE%</i> (%)	<i>SD</i> (km/s)	<i>MSE</i> (km/s)	<i>RMSE</i> (km/s)	<i>R²</i> -
<i>Pickett</i>	3.493	4.373	0.1433	0.0206	0.1434	0.8643
<i>Castagna et al.</i>	1.953	3.628	0.1224	0.0150	0.1224	0.8628
<i>Eskandari et al.</i>	2.265	4.033	0.1336	0.0178	0.1335	0.8507
<i>Brocher</i>	-4.115	7.352	0.1987	0.0395	0.1988	0.8634
<i>MLP</i>	-0.338	1.812	0.0701	0.0049	0.0701	0.9544
<i>ELM</i>	-0.205	1.628	0.0517	0.0027	0.0518	0.9730

Table 8. Accuracy achieves for shear wave velocity prediction applied to the total dataset (100% of the dataset).

<i>Models Unit</i>	<i>ARE%</i> (%)	<i>AARE%</i> (%)	<i>SD</i> (km/s)	<i>MSE</i> (km/s)	<i>RMSE</i> (km/s)	<i>R²</i> -
<i>Pickett</i>	3.945	4.863	0.1524	0.0233	0.1525	0.8545
<i>Castagna et al.</i>	2.299	3.977	0.1286	0.0165	0.1286	0.8542
<i>Eskandari et al.</i>	2.607	4.351	0.1382	0.0191	0.1381	0.8436
<i>Brocher</i>	-4.221	7.637	0.2028	0.0411	0.2028	0.8545
<i>MLP</i>	-0.212	1.618	0.0553	0.0031	0.0554	0.9676
<i>ELM</i>	-0.121	1.434	0.0445	0.0020	0.0444	0.9809

Figure 6 shows the values of two very important criteria for regression (RMSE and R²) of artificial intelligence models and experimental equations to predict shear wave velocity. As shown in this figure, the performance accuracy of ELM is much higher than other models of artificial intelligence experimental equations. In other words, performance accuracy can be expressed for artificial intelligence models and experimental equations as follows: ELM > MLP > Castagna et al. > Eskandari et al. > Pickett > Brocher.

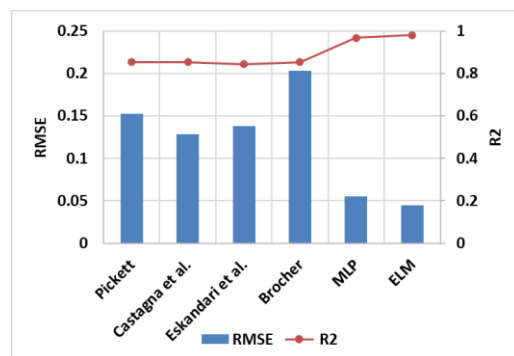


Figure 6. Determination of RMSE and R² for four empirical equations (Brocher, Eskandari et al., Castagna et al. and Pickett) and two machine learning models (ELM and MLP) models (ELM and MLP)

Figures 7 and 8 show the Predicted versus measured shear wave velocity (Km / s) values for the total data values of the #A and #B wells. These figures show that the ELM model performs better than other empirical equations and the MLP model. In addition, as it turns out, this algorithm has more power in preventing outlier data. The ELM model's highest shear wave velocity prediction accuracy applied to all 1909 data records were RMSE= 0.0444 and $R^2 = 0.9809$.

As mentioned in the methods It is claimed that this approach is fast and less time consuming This word fast means run time. As shown in Tables 9 and 10, ELM is much faster than MLP. Table 9 provides run time information for #A and #B wells training and testing data, and Table 10 provides run time validation information for #C wells.

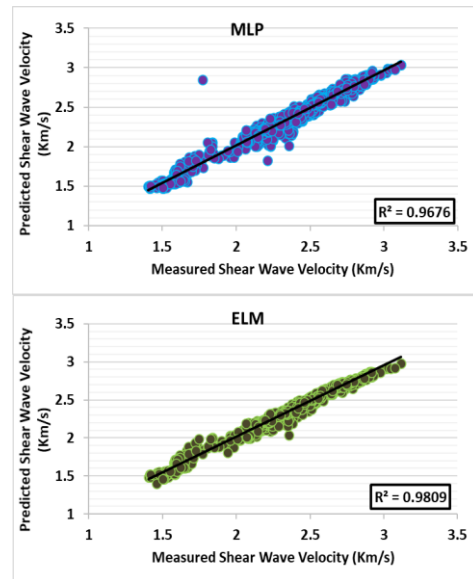


Figure 7. Predicted/Measured shear wave velocity comparisons for the machine-learning model (ELM/ MLP) applied to the complete well #A and #B dataset of 1909 data records.

Table 9. Computer run time for #A and #B well.

<i>Training (s)</i>		<i>Testing (s)</i>	
<i>MLP</i>	<i>ELM</i>	<i>MLP</i>	<i>ELM</i>
98.74	66.39	23.16	14.25

Table 10. Computer run time for #C well. This well is only used model validation.

<i>Training (s)</i>		<i>Validation (s)</i>	
<i>MLP</i>	<i>ELM</i>	<i>MLP</i>	<i>ELM</i>
N/A	N/A	21.47	12.68

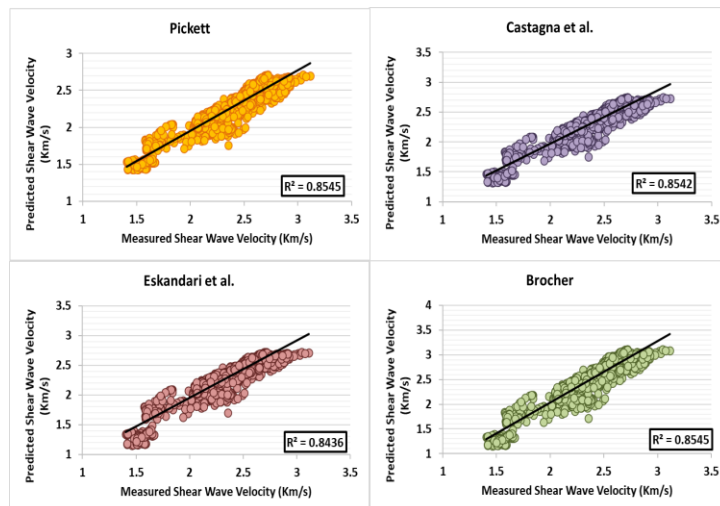


Figure 8. Predicted/Measured shear wave velocity comparisons for the empirical equation model (Brocher/ Eskandari et al./ Castagna et al./ Pickett) applied to the complete well #A and #B dataset of 1909 data records.

4.6. Data Validation for ELM Model

Based on the results from the information related to #A and #B wells to predict shear wave velocity using 4 inputs from the feature selection method, it was determined that the ELM algorithm has higher performance accuracy than other models and MLP. Then, to validate the presentation algorithm, in this paper, information about the #C well (971 data records) from the same field is used, the results of which are presented in Table 11 and Figure 9.

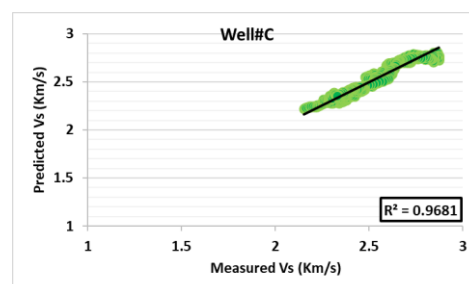


Figure 9. Predicted/Measured shear wave velocity comparisons for the ELM model applied to the complete well #C dataset of 971 data records.

Table 11. Validation of ELM algorithm based on well #A and #B to shear wave velocity prediction for complete datasets of well #C.

<i>Models</i>	<i>ARE%</i>	<i>AARE%</i>	<i>SD</i>	<i>MSE</i>	<i>RMSE</i>	<i>R²</i>
<i>Unit</i>	(%)	(%)	(km/s)	(km/s)	(km/s)	-
<i>well #C</i>	-0.035	1.624	0.0533	0.00285	0.0534	0.9681

According to the results of Table 8 and Figure 9, it can be concluded that this highly available and high-performance algorithm can be used for other wells and even other fields. Therefore, this is a suitable, fast, easy and low-cost solution to determine this parameter.

5. Conclusion

In this paper, we used two machine learning models (ELM and MLP) and four empirical equations (Brocher, Eskandari et al., Castagna et al. and Pickett) for shear wave velocity prediction based on three wells (well #A, #B and #C) of one of the oil fields in southwest of Iran. To create machine learning modes, two well #A and #B (1909 dataset) were used to validate the best model used well #C (971 datasets).

The algorithm ELM used in this study has a novel algorithm that has some advantages to another artificial neural network: good accuracy and performance characteristics, simple algorithm learning, improved performance, nonlinear conversion during training, and no stuck in local optimal points is

overfitting. These advantages caused this algorithm to separate from the other algorithms.

Between eight input variables that used in this study; neutron porosity (NPHI); bulk density (RHOB); shallow resistivity (RES-SHT); compressional-wave velocity (V_p); medium resistivity (RES-MED); gamma-ray (GR); deep resistivity (RES-DEP) and caliper (CP), after feature selection found four input variables (V_p, RHOB, NPHI and GR) have best the combination of input variables.

After dividing the data into two parts, training and testing, and after comparing artificial intelligence algorithms (MLP and ELM) and empirical equations (Brocher, Eskandari et al., Castagna et al. And Pickett), it was finally concluded that follows: ELM > MLP > Castagna et al. > Eskandari et al. > Pickett > Brocher.

To validate the ELM algorithm for other wells and other fields, the #C well is nominated for this purpose. Its results show that the performance accuracy of this algorithm is high and can be used for other wells

6. Acknowledgement

The authors are grateful to Ms. Fatemeh Kalaei for his technical support and efforts in collecting the data needed for this study

Conflicts of Interest

The authors declare that they have no conflicts of interest regarding the material included in this manuscript.

Nomenclature

<i>AARE</i>	=	<i>Average absolute relative error</i>
<i>ANFIS</i>	=	<i>Adaptive neuro-fuzzy inference</i>
<i>ANN</i>	=	<i>Artificial neural network</i>
<i>ARE</i>	=	<i>Average relative error</i>
<i>COA</i>	=	<i>Cuckoo optimization algorithm</i>
<i>DSI</i>	=	<i>Sonic dipole log</i>
<i>ELM</i>	=	<i>Extra learning machine</i>
<i>ENN</i>	=	<i>Elman neural network</i>
<i>FL</i>	=	<i>Fuzzy logic</i>
<i>GA</i>	=	<i>Genetic algorithm</i>
<i>GR</i>	=	<i>Gamma-ray</i>
<i>GRG</i>	=	<i>Generalized reduced gradient</i>
<i>LSSVM</i>	=	<i>Least-squares support-vector machines</i>
<i>MLP</i>	=	<i>Multi-layer perceptron</i>
<i>MSE</i>	=	<i>Mean square error</i>
<i>NPFI</i>	=	<i>Neutron porosity</i>
<i>PDi</i>	=	<i>Percentage deviation</i>
<i>PEF</i>	=	<i>Photoelectric absorption factor</i>
<i>R²</i>	=	<i>Coefficient of determination</i>
<i>RHOB</i>	=	<i>Bulk density</i>
<i>RMSE</i>	=	<i>Root mean square error</i>
<i>RS</i>	=	<i>Shallow resistivity</i>
<i>RT</i>	=	<i>True resistivity</i>
<i>SD</i>	=	<i>Standard deviation</i>
<i>SVR</i>	=	<i>Support vector regression</i>
<i>TOB</i>	=	<i>Transparent open box</i>
<i>V_p</i>	=	<i>Compressional wave velocity</i>
<i>V_s</i>	=	<i>Shear wave velocity</i>

References

- Akhundi, H., Ghafoori, M., Lashkaripour, G.-R., 2014. Prediction of shear wave velocity using artificial neural network technique, multiple regression and petrophysical data: A case study in Asmari reservoir (SW Iran). *Open Journal of Geology* 2014. doi: <http://creativecommons.org/licenses/by/4.0/>
- Ali, J., 1994. Neural networks: a new tool for the petroleum industry?, *European petroleum computer conference*. Society of Petroleum Engineers. doi: <https://doi.org/10.2118/27561-MS>.
- Anemangely, M., Ramezanzadeh ,A., Amiri, H., Hoseinpour, S.-A., 2019. Machine learning technique for the prediction of shear wave velocity using petrophysical logs. *Journal of Petroleum Science and Engineering* 174, 306-327. doi: <https://doi.org/10.1016/j.petrol.2018.11.032>.
- Bagheripour, P., Gholami, A., Asoodeh, M., Vaezzadeh-Asadi, M., 2015. Support vector regression based determination of shear wave velocity. *Journal of Petroleum Science and Engineering* 125, 95-99. doi: <https://doi.org/10.1016/j.petrol.2014.11.025>

Behnia, D., Ahangari, K., Moeinossadat, S.R., 2017. Modeling of shear wave velocity in limestone by soft computing methods. *International Journal of Mining Science and Technology* 27, 423-430. doi: <https://doi.org/10.1016/j.ijmst.2017.03.006>.

Cheng, J., Xiong, Y., 2017 .Application of extreme learning machine combination model for dam displacement prediction. *Procedia Computer Science* 107, 373-378. doi: <https://doi.org/10.1016/j.procs.2017.03.120>.

Choubineh, A., Ghorbani, H., Wood, D.A., Moosavi, S.R., Khalafi, E., Sadatshojaei, E., 2017. Improved predictions of wellhead choke liquid critical-flow rates: modelling based on hybrid neural network training learning based optimization. *Fuel* 207, 547-560. doi: <https://doi.org/10.1016/j.fuel.2017.06.131>.

Du, Q., Yasin, Q., Ismail, A., Sohail, G.M., 2019. Combining classification and regression for improving shear wave velocity estimation from well logs data. *Journal of Petroleum Science and Engineering* 182, 106260. doi: <https://doi.org/10.1016/j.petrol.2019.106260>.

Elkhatatny ,S., Mahmoud, M., Mohamed, I., Abdulraheem, A., 2018. Development of a new correlation to determine the static Young's modulus. *Journal of Petroleum Exploration and Production Technology* 8, 17-30. doi: <https://link.springer.com/article/10.1007/s13202-017-0431-6>

Ghorbani, H., Moghadasi, J., Wood, D.A., 2017. Prediction of gas flow rates from gas condensate reservoirs through wellhead chokes using a firefly optimization algorithm. *Journal of Natural Gas Science and Engineering* 45, 256-271. doi: <https://doi.org/10.1016/j.jngse.2017.04.034>.

Ghorbani, H., Wood, D.A., Choubineh, A., Mohamadian, N., Tatar, A., Farhangian, H., Nikooy, A., 2020. Performance comparison of bubble point pressure from oil PVT data: Several neurocomputing techniques compared. *Experimental and Computational Multiphase Flow* 2, 225-246. doi: <https://link.springer.com/article/10.1007/s42757-019-0047-5>.

Ghorbani, H., Wood, D.A., Choubineh, A., Tatar, A., Abarghoyi, P.G., Madani, M., Mohamadian, N., 2018. Prediction of oil flow rate through an orifice flow meter: Artificial intelligence alternatives compared. *Petroleum*. doi: <https://doi.org/10.1016/j.petlm.2018.09.003>.

Ghorbani, H., Wood, D.A., Moghadasi, J., Choubineh, A., Abdizadeh, P., Mohamadian, N., 2019. Predicting liquid flow-rate performance through wellhead chokes with genetic and solver optimizers: an oil field case study. *Journal of Petroleum Exploration and Production Technology* 9, 1355-1373. doi: <https://link.springer.com/article/10.1007/s13202-018-0532-6>.

Huang, G.-B., 2014. An insight into extreme learning machines: random neurons, random features and kernels. *Cognitive Computation* 6, 376-390. doi: <https://link.springer.com/article/10.1007%2Fs12559-014-9255-2>.

Huang, G.-B., Zhou, H., Ding, X., Zhang, R., 2011. Extreme learning machine for regression and multiclass classification. *IEEE Transactions on Systems, Man, and Cybernetics, Part B (Cybernetics)* 42, 513-529. doi: <https://doi.org/10.1109/TSMCB.2011.2168604>.

Hudson, J.A., Stephansson, O., Andersson, J., 2005. Guidance on numerical modelling of thermo-hydro-mechanical coupled processes for performance assessment of radioactive waste repositories. *International Journal of Rock Mechanics and Mining Sciences* 42, 850-870. doi: <https://doi.org/10.1016/j.ijrmms.2005.03.018>.

Kaviani-Hamedani, F., Fakharian, K., Lashkari, A., 2021. Bidirectional shear wave velocity measurements to track fabric anisotropy evolution of a crushed silica sand during shearing. *Journal of Geotechnical and*

Geoenvironmental Engineering 147, 04021104. doi :<https://orcid.org/0000-0001-6153-2877>.

Khoshouei, M., Bagherpour, R., 2021. Predicting the Geomechanical Properties of Hard Rocks Using Analysis of the Acoustic and Vibration Signals During the Drilling Operation. *Geotechnical and Geological Engineering* ۲۰۹۹-۲۰۸۷, ۳۹ doi: <https://link.springer.com/article/10.1007/s10706-020-01611-z>.

Mehrgini, B., Izadi, H., Memarian, H., 2019. Shear wave velocity prediction using Elman artificial neural network. *Carbonates and Evaporites* 34, 1281-1291. doi: <https://link.springer.com/article/10.1007/s13146-017-0406-x>.

Miah, M.I., Ahmed, S., Zendeboudi, S., 2021. Model development for shear sonic velocity using geophysical log data: Sensitivity analysis and statistical assessment. *Journal of Natural Gas Science and Engineering* 88, 103778. doi: <https://doi.org/10.1016/j.jngse.2020.103778>.

Mohamadian, N., Ghorbani, H., Wood, D.A., Mehrad, M., Davoodi, S., Rashidi, S., Soleimani, A., Shahvand, A.K., 2021. A geomechanical approach to casing collapse prediction in oil and gas wells aided by machine learning. *Journal of Petroleum Science and Engineering* 196, 107811. doi: <https://doi.org/10.1016/j.petrol.2020.107811>.

Najibi, A.R., Ghafoori, M., Lashkaripour, G.R., Asef, M.R., 2015. Empirical relations between strength and static and dynamic elastic properties of Asmari and Sarvak limestones, two main oil reservoirs in Iran. *Journal of Petroleum Science and Engineering* 126, 78-82. doi: <https://doi.org/10.1016/j.petrol.2014.12.010>.

Oloruntobi, O., Butt, S., 2020. The shear-wave velocity prediction for sedimentary rocks. *Journal of Natural Gas Science and Engineering* 76, 103084. doi: <https://doi.org/10.1016/j.jngse.2019.103084>.

Parvizi, S., Kharrat, R., Asef, M.R., Jahangiry, B., Hashemi, A., 2015. Prediction of the shear wave velocity from compressional wave velocity for Gachsaran Formation. *Acta Geophysica* 63, 1231-1243. doi: <https://link.springer.com/article/10.1515/acgeo-2015-0048>.

Rajabi, M., Bohloli, B., Ahangar, E.G., 2010. Intelligent approaches for prediction of compressional, shear and Stoneley wave velocities from conventional well log data: A case study from the Sarvak carbonate reservoir in the Abadan Plain (Southwestern Iran). *Computers & Geosciences* 36, 647-664. doi: <https://doi.org/10.1016/j.cageo.2009.09.008>.

Rashidi, S., Mehrad, M., Ghorbani, H., Wood, D.A., Mohamadian, N., Moghadasi, J., Davoodi, S., 2021. Determination of bubble point pressure & oil formation volume factor of crude oils applying multiple hidden layers extreme learning machine algorithms. *Journal of Petroleum Science and Engineering*, 108425. doi: <https://doi.org/10.1016/j.petrol.2021.108425>.

Rezaee, M.R., Ilkhchi, A.K., Barabadi, A., 2007. Prediction of shear wave velocity from petrophysical data utilizing intelligent systems: An example from a sandstone reservoir of Carnarvon Basin, Australia. *Journal of Petroleum Science and Engineering* 55, 201-212. doi: <https://doi.org/10.1016/j.petrol.2006.08.008>.

Rhett, D.W., 1998. Ekofisk revisited: a new model of Ekofisk reservoir geomechanical behavior. *OnePetro*. doi: <https://onepetro.org/conference-paper/SPE-47273-MS>.

Seifi, H., Tokhmechi, B., Moradzadeh, A., 2020. Improved estimation of shear-wave velocity by ordered weighted averaging of rock physics models in a carbonate reservoir. *Natural Resources Research* 29, 2599-2617. doi: <https://link.springer.com/article/10.1007/s11053-019-09590-6>.

Sohail, G.M., Hawkes, C.D., 2020. An evaluation of empirical and rock physics models to estimate shear wave velocity in a potential shale gas reservoir using wireline logs. *Journal of Petroleum Science and*

Engineering 185, 106666. doi: <https://doi.org/10.1016/j.petrol.2019.106666>.

Sohail, G.M., Hawkes, C.D., Yasin, Q., 2020. An integrated petrophysical and geomechanical characterization of Sembar Shale in the Lower Indus Basin, Pakistan, using well logs and seismic data. *Journal of Natural Gas Science and Engineering* 78, 103327. doi: <https://doi.org/10.1016/j.jngse.2020.103327>.

Tixier, M.P., Loveless, G.W., Anderson, R.A., 1975. Estimation of formation strength from the mechanical-properties log (includes associated paper 6400). *Journal of Petroleum Technology* 27, 283-293. doi: <https://doi.org/10.2118/4532-PA>.

Wang, H.F., 2000. *Linear poroelasticity*. Princeton, NJ: Princeton University Press.

Wang, J., Cao, J., Yuan, S., 2020. Shear wave velocity prediction based on adaptive particle swarm optimization optimized recurrent neural network. *Journal of Petroleum Science and Engineering* 194, 107466. doi: <https://doi.org/10.1016/j.petrol.2020.107466>.

Wang, J., Wu, S., Zhao, L., Wang, W., Wei, J., Sun, J., 2019. An effective method for shear-wave velocity prediction in sandstones. *Marine Geophysical Research* 40, 655-664. doi: <https://link.springer.com/article/10.1007/s11001-019-09396-4>.

Wood, D.A., 2020. Bakken stratigraphic and type well log learning network exploited to predict and data mine shear wave acoustic velocity. *Journal of Applied Geophysics* 173, 103936. doi: <https://doi.org/10.1016/j.jappgeo.2019.103936>.

Yeom, C.-U., Kwak, K.-C., 2017. Short-term electricity-load forecasting using a TSK-based extreme learning machine with knowledge representation. *Energies* 10, 1613. doi: <https://doi.org/10.3390/en10101613>.